Maximally-localized Wannier functions for a two-dimensional electron gas in a periodic potential

David Haag

Lund University

May, 2026: Project duration one semester, half time, 15 ECTS

Supervisor: Erik van Loon, Yiqi Yang

Department of Physics

Bachelor thesis

Contents

Abstract

This project concerns the Wannier functions of a two-dimensional electron gas within a simple periodic lattice. Wannier functions are an exponentially localized basis for electron bands and allow for real-space calculations of interacting electron systems. These functions are not unique; using the Wannier functions with minimal spatial spread is the standard in research. In this thesis, the maximally localized Wannier functions were calculated using a gradient descent algorithm. Wannier functions for a non-interacting system were computed and compared to the equivalent functions computed from an existing density functional theory data set with different electron-electron interaction strengths. The density function theory Wannier functions showed only minor differences from the non-interacting model. The functions slightly widened, resulting in an 11% increase in the spread for the Wannier function with the strongest Coulomb interaction. The difference observed could be well described as a perturbation of the Wannier functions scaled by a parameter dependent on the Coulomb strength.

I. INTRODUCTION

The properties of solids arise from the interplay between the electronic, atomic and magnetic degrees of freedom. The electrons are responsible for important properties such as electrical conductivity, heat conductivity, and optical properties. It is often possible to treat atoms classically, while the small mass of the electron necessitates quantum mechanics. Furthermore, the strength of the Coulomb interaction is generally large. This represents a many-body quantum system where electron-lattice and electron-electron interactions need to be accounted for, and theoretical solutions rarely exist, creating a need for approximations.

The creation of real systems serving as quantum simulators that replicate model conditions can solve computationally difficult many-body problems and can be used for tuning future theoretical models. In general, real materials are imperfect; they have lattice irregularities and impurities, making them unsuitable for this purpose. Previous research on simulating materials has focused on optical lattices and ultra-cold gases, avoiding the need for solids[1]. Advancements in two-dimensional materials have led to them being proposed as another simulator for electrons in a lattice.

The first two-dimensional material, graphene, was isolated by Geim and Novoselov through mechanical exfoliation of graphite[2], stripping away layers until a single layer of carbon remained. Graphene has extremely high tensile strength, large carrier mobility, and demonstrates novel experimental quantum effects. An intensive period of research into graphene and other mono-layered crystals followed. Each material provides a unique two-dimensional environment.

However, the number of viable materials is limited as the formation of a stable monolayer is rare. Stacking different two-dimensional crystals expands the possibilities significantly. The sheets are weakly bound by Van der Waals forces, allowing for the creation of new three-dimensional structures. These Van der Waals heterostructures[3] can be engineered to have specific electronic properties.

The introduction of a mismatch of angles or lattice constants between layers creates a new periodic structure, analogous to a moiré pattern, with length scales much greater than the underlying lattices. A subset of these systems can be effectively described by a potential with the same long-range periodicity as the lattice; these are called moiré potentials. Such systems have been proposed as effective quantum simulators for a two-dimensional electron gas in a lattice[4].

A major difference between two-dimensional and three-dimensional materials is the role of the environment. Conventional three-dimensional materials have their surface affected by neighboring fields, while the bulk is unaffected; the internal electron environment is, in part, a fixed material property. Two-dimensional structures are just a surface, meaning the entire system is affected. For moiré potentials, the source can be other layers in the heterostructure; an experimental system can thus be engineered when building the material. The introduction of metallic substrates on both sides acts as screening gates, reducing the Coulomb interaction between electrons. The strength of the screening depends on the distance to the gates, allowing for the parametrization of correlation and interaction effects.

In the present work, the case of a square lattice is considered. Unlike the triangular lattice, this moiré pattern has not been realized in practice, and simulation tools will be used. An existing dataset for interacting electrons in a square lattice with different screening strengths computed using density functional theory will be compared with the results of a non-interacting model created for this thesis.

II. Theory

II.A. Periodic potentials and Bloch states

Bloch's theorem is essential for the description of electrons in solids. It allows for the discreet translational symmetry in a crystal to be used to simplify the Schrödinger equation. Here, we study the time-independent Schrödinger equation for independent electrons in the presence

of a periodic potential. It takes the form

$$E\left|\psi\right\rangle = -\frac{\hbar^2}{2m}\nabla^2\left|\psi\right\rangle + V(\boldsymbol{r})\left|\psi\right\rangle, \tag{1}$$
$$V(\boldsymbol{r}+\boldsymbol{R}) = V(\boldsymbol{r}),$$

where $\boldsymbol{R}$ is a translation vector of the relevant Bravais lattice. For the square lattice the two translation vectors are $\boldsymbol{R} = (a, 0)$ and $\boldsymbol{R} = (0, a)$.
Bloch's theorem says solutions take the form

$$\psi_{n\boldsymbol{k}}(\boldsymbol{r}) = u_{n\boldsymbol{k}}(\boldsymbol{r})\ e^{-i\boldsymbol{k}\boldsymbol{r}}, \tag{2}$$
$$u_{n\boldsymbol{k}}(\boldsymbol{r}+\boldsymbol{R}) = u_{n\boldsymbol{k}}(\boldsymbol{r}). \tag{3}$$

$\boldsymbol{k}$ is a wave vector belong to the Brillouin zone and n is the band index. The Bloch states in the first Brillouin zone form a complete basis for the solution space to Eq (1), so determining $u_{n\boldsymbol{k}}$ and the energies for each $\boldsymbol{k}$ describes the entire physical system and gives the band structure. This formulation will be used in the numerical methods in this project. For the relevant square lattice, the Brillouin zone is a square centered at a reciprocal lattice point with side length $\frac{2\pi}{a}$.

Expanding Eq (2) using a Fourier series gives a set of basis functions for each $\boldsymbol{k}$ which can be used to express the Hamiltonian,

$$\begin{aligned}\hat{H}^{(\boldsymbol{k})}_{\boldsymbol{G}\boldsymbol{G'}} &= \langle u_{\boldsymbol{G}\boldsymbol{k}}|\hat{H}|u_{\boldsymbol{G'}\boldsymbol{k}}\rangle, \\ &= \frac{\hbar^2}{2m}(\boldsymbol{G}+\boldsymbol{k})^2\delta_{\boldsymbol{G}\boldsymbol{G'}} + \hat{V}(\boldsymbol{G}-\boldsymbol{G'}).\end{aligned} \tag{4}$$

$\hat{\boldsymbol{V}}$ is the Fourier series of the potential, $\boldsymbol{G}$ and $\boldsymbol{G'}$ are vectors storing the Fourier series indices. A simple example of a one-dimensional band structure computed using Eq (4) is shown below.

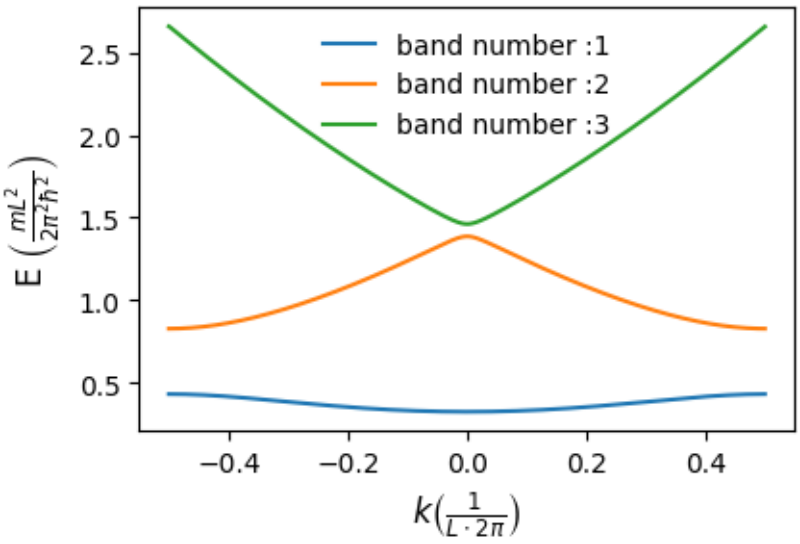

Figure I: Eigenenergies for 1d system with $V(x) = 0.4\left(1 - \cos(x\frac{2\pi}{L})\right)$.

Figure (I) shows the three smallest eigenvalues plotted over a unit cell in k-space, L is the length of a unit cell, V_0 has energy units of $\frac{mL^2}{2\pi^2\hbar^2}$. The first band gap is located at the edge of the reciprocal unit cell with a size of $\approx V_0$, and the second at the center with a size of $\approx V_0^2$. In the nearly free electron model, where the potential is treated as perturbing free electrons, these approximations are the exact values of the band gaps.

II.B. Wannier functions

The Bloch states discussed so far have the advantage of being easily computable, but they are delocalized over all of $\mathbb{R}^n$. Wannier functions are an alternative basis. They are exponentially localized with one function per band per unit cell[5]. Wannier functions are similar to atomic orbitals and show analogous symmetries. The purpose of this project is to calculate Wannier functions and characterize their localization for the square lattice cosine potential.

A set of Wannier functions is computed from and span a set of bands; each choice of bands gives a set of Wannier functions. To construct the Wannier functions, the gauge freedom in the Bloch states for the relevant bands is needed. For a set of N overlapping bands $\{|\psi_{n\boldsymbol{k}}\rangle, n \in N\}$ an $N \times N$ unitary matrix, $U^{(\boldsymbol{k})}_{n,m}$, defines another valid basis

$$|\hat{\psi}_{m\boldsymbol{k}}\rangle = U^{(\boldsymbol{k})}_{n,m} |\psi_{n\boldsymbol{k}}\rangle . \tag{5}$$

The choice of gauge changes how smooth $|\psi_{n\boldsymbol{k}}\rangle$ are in $\boldsymbol{k}$.

For each lattice point R, the Wannier function for a set of bands is

$$|R_m\rangle = \int_{BZ} d\boldsymbol{k} \frac{V_{BZ}}{(2\pi)^n} e^{-i\boldsymbol{k}\cdot\boldsymbol{R}} U^{(\boldsymbol{k})}_{n,m} |\psi_{n\boldsymbol{k}}\rangle \,. \tag{6}$$

This transformation maps N bands to N functions repeated for every unit cell and is invertible. For gauges with a high degree of smoothness in $\boldsymbol{k}$, each Wannier function is exponentially decaying around its central lattice point.

The freedom in $U^{(\boldsymbol{k})}_{n,m}$ means that the exact gauge is often a consequence of the computation method used for the Bloch states and can be highly irregular. To measure the suitability of a given gauge, the Marzari-Vanderbilt localization functional introduced in [6] is commonly used. It returns the sum of the spread of the Wannier functions and is

$$\Omega_1 = \sum_n [\langle \mathbf{0}_n | r^2 | \mathbf{0}_n \rangle - \langle \mathbf{0}_n | \boldsymbol{r} | \mathbf{0}_n \rangle^2]. \tag{7}$$

$|0_n\rangle$ is the n-th Wannier function for the central lattice point. A global minima to Eq (7) is thus the optimal choice when considering spatial extent, such functions are called maximally localized Wannier functions.

The question of the existence of a U where $|R_n\rangle$ decays exponentially is not solved for the most general case in 3 dimensions; [7] provides an outline of the current results. Relevant for this project is that gauges that minimize Eq (7) exist and are exponentially decaying for $d \leq 2$.

III. Method

III.A. Non interacting model

A numerical model was implemented for solving the Hamiltonian

$$\hat{H} = -\nabla^2 + 2V_0 \Big(\cos(x) + (\cos(y) \Big), \tag{8}$$

given with units setting $\hbar = 1$, $m = 1$ and $a = 2\pi$. By diagonalizing a finite subset of the matrix representation from Eq (4), the wave functions and eigenenergies were computed using standard linear algebra tools.

Through the entire project, a $\boldsymbol{k}$-grid with dimension 30×30 was used. For the Hamiltonian the plane waves $|u_{\boldsymbol{Gk}}\rangle$ were restricted to values with $|k_x|$ and $|k_y| \leq 5$. The resulting band structure is shown below.

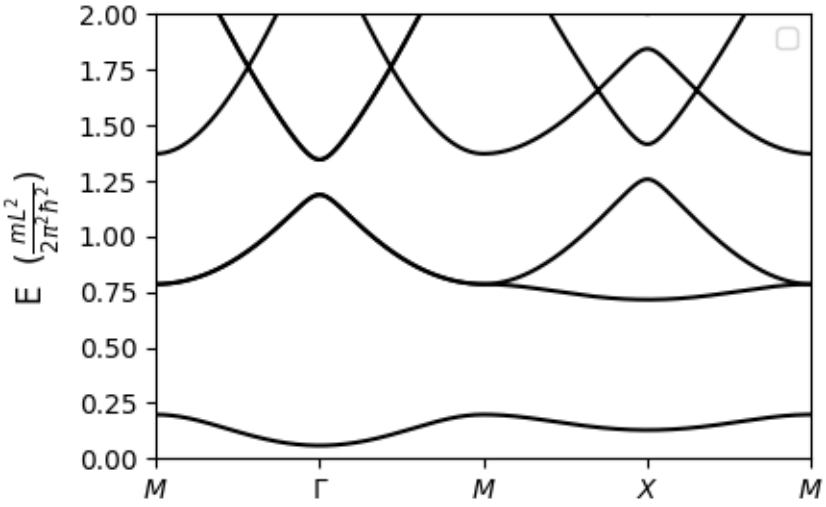

Figure II: Bands for Hamiltonian in Eq (8).

The path used in Figure(II) crossed the points $M = (0.5, 0.5)$, $\Gamma = (0, 0)$ and $X = (0, 0.5)$.

III.B. Maximally localized Wannier functions

To find the gauge minimizing Eq (7) for a given set of Bloch bands, a gradient descent algorithm was implemented. A first-order finite difference expression for the gradient of the localization operator was introduced in [6]. It uses the fact that the expectation values of position and position squared of the Wannier functions are computable from the Bloch states by

$$\langle \boldsymbol{r} \rangle_n = i \frac{V}{2\pi^d} \int d\boldsymbol{k} \, \langle u_{n\boldsymbol{k}} | \nabla_{\boldsymbol{k}} | u_{n\boldsymbol{k}} \rangle \,, \tag{9}$$

$$\langle \boldsymbol{r^2} \rangle_n = -\frac{V}{2\pi^d} \int d\boldsymbol{k} \, \langle u_{n\boldsymbol{k}} | \nabla^2_{\boldsymbol{k}} | u_{n\boldsymbol{k}} \rangle \,. \tag{10}$$

These can be estimated using finite differences, and from these, an algorithm for the gradient is derived. The resulting gradient, $G^{(\boldsymbol{k})}$, is an anti-Hermitian matrix, and the gauge is updated with step size α according to

$$U^{(\boldsymbol{k})}_{\text{new}} = U^{(\boldsymbol{k})}_{\text{old}} \exp(\alpha G^{(\boldsymbol{k})}). \tag{11}$$

The algorithm terminated when $G^{(k)}$ became sufficiently small as measured with the sum of its squared entries.

III.C. Density functional theory

This work relies on a preexisting data set for Wannier functions computed for an interacting electron gas with screening from metallic gates; the screening is parameterized by the separation d. As $d \to 0$, this becomes the model from EQ 8, comparing them shows the effect of electron-electron interactions. The relevant Hamiltonian becomes in effective Hartree and effective Bohr radii

$$\begin{aligned} \hat{H} =& -\frac{1}{2r_s^2}\sum_{i=1}\tilde{\nabla}_i^2 + \frac{1}{2r_s^2}\sum_{i\neq j} v(|\tilde{\boldsymbol{r}}_i - \tilde{\boldsymbol{r}}_j|, d) \\ & - V_m \sum \Lambda(\tilde{\boldsymbol{r}}_i) + V_{\text{background}}, \\ \Lambda(\boldsymbol{r}) =& 2\Big(\cos(x|\boldsymbol{b}|)) + (\cos(y|\boldsymbol{b}|)\Big). \end{aligned} \tag{12}$$

v is the screened electron-electron interaction, $V_{\text{background}}$ is the background potential of the electron gas, r_s is the Wigner-Seitz radius of an electron gas with the same electron density, one particle per unit cell. $\tilde{\boldsymbol{r}}$ is the ratio between $\boldsymbol{r}$ and r_s. The potential is a first-order harmonic approximation over the reciprocal unit vectors $\boldsymbol{b}$. The system is parameterized by d and the energy scale

$$\epsilon = V_m \cdot r_s^2. \tag{13}$$

This can be matched to potential depth in Eq 8 by

$$V_0 = \frac{\epsilon}{2\pi}. \tag{14}$$

This follows from r_s being the Wigner-Seitz radius for a gas with one electron per unit cell. The parameter space used was a constant energy scale of $\epsilon = 1.4$ and a separation of $d \in \{\, 0.1, 0.2, 0.4, 0.6, 0.9 \,\}$ with units of r_s. As $d \to 0$, the Coulomb interaction goes to zero and the non-interacting model is expected to give matching results.

IV. RESULTS

IV.A. Non-interacting model

The numeric model successfully produces maximally localized Wannier functions for multiple bands over a wide range of ϵ.

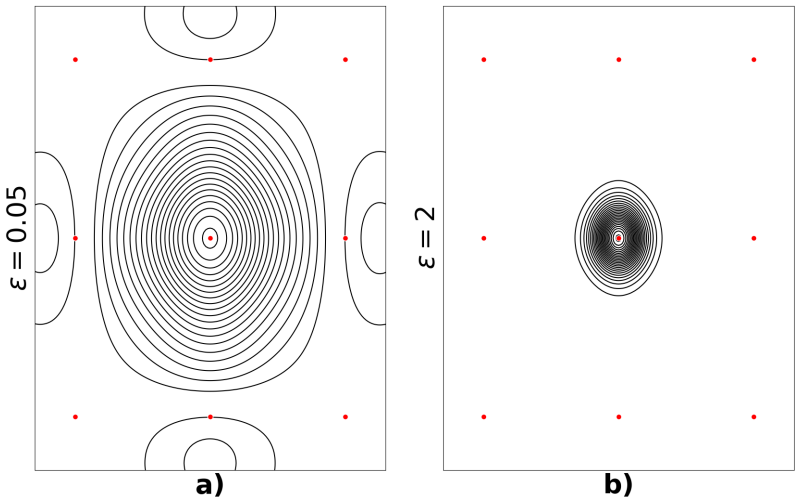

Figure III: Ground state Wannier contours for a shallow and deep for Eq (8).

Figure(III) shows the contour for 2 Wannier functions for different potentials. They are centered at the origin and shown over a 3×3 square of unit cells. In ***a)*** a small potential was used, and ***b***) shows a deep potential. In the large limit of ϵ, the solution is very localized and shows circular symmetry. This is the symmetry of a two-dimensional harmonic oscillator, which is the second-order Taylor expansion of the used potential, $\cos(x) \approx 1 - \frac{1}{2}x^2$. For small ϵ, the wave functions start to bleed out to the closest neighboring unit cells and have the same fourfold symmetry as the potential.

The localization functional from Eq (7) can be used to quantify the relation between spatial extent and the gate separation d.

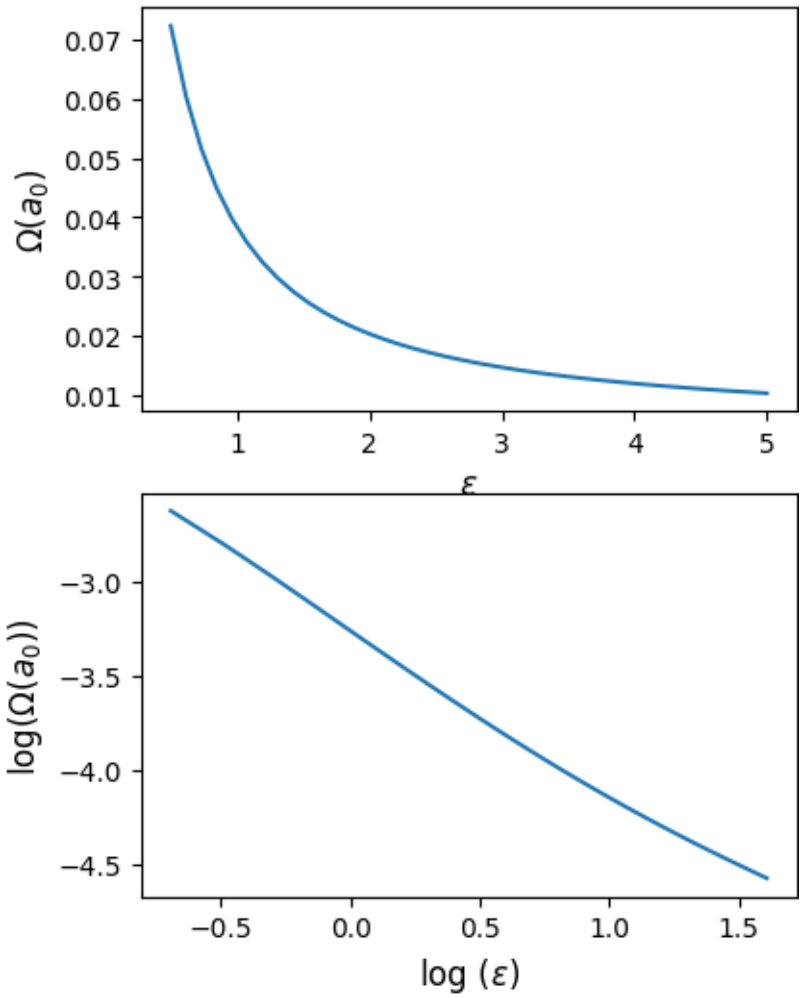

Figure IV: Marzari-Vanderbilt functional for maximally localized Wannier with different values of $\epsilon = V_0 \cdot 2\pi$.

Figure (IV) shows Ω_1 decaying over a range of energy scales, the relation is well described by $\Omega_1 \propto \frac{1}{\epsilon}$ as shown in the log-log plot.

IV.B. DFT and non-interacting comparison

To quantify the dependence of d on the ground state Wannier functions, the spread functional from Eq (7) is an important tool. Labeling the non-interacting model as $d = 0$ shows that increasing Coulomb repulsion makes the electrons spread out more.

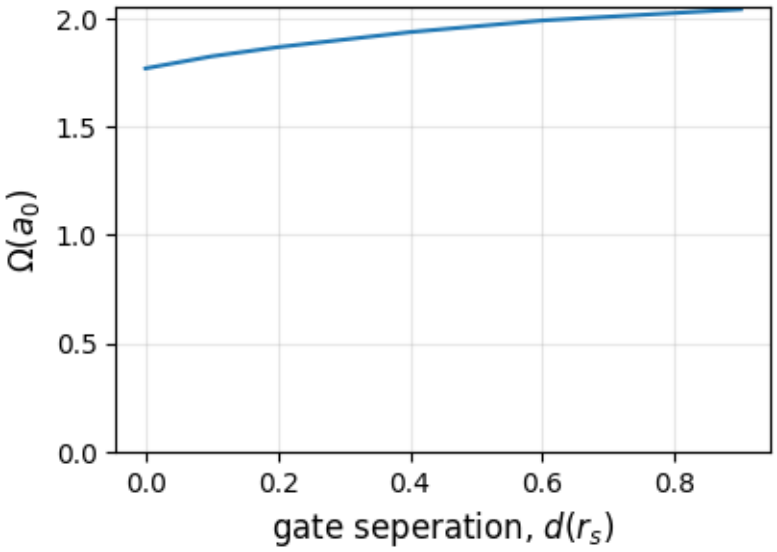

Figure V: Spread of the Wannier functions over the metallic gate screening distance d.

Figure (V) shows how, as the separation d increases and the electron-electron interaction strengthens, the spread grows, indicating a slight widening of the Wannier functions. Subtracting the non-interacting ground state from the interacting states shows the spatial difference. This is shown along a line cut along the y-axis below.

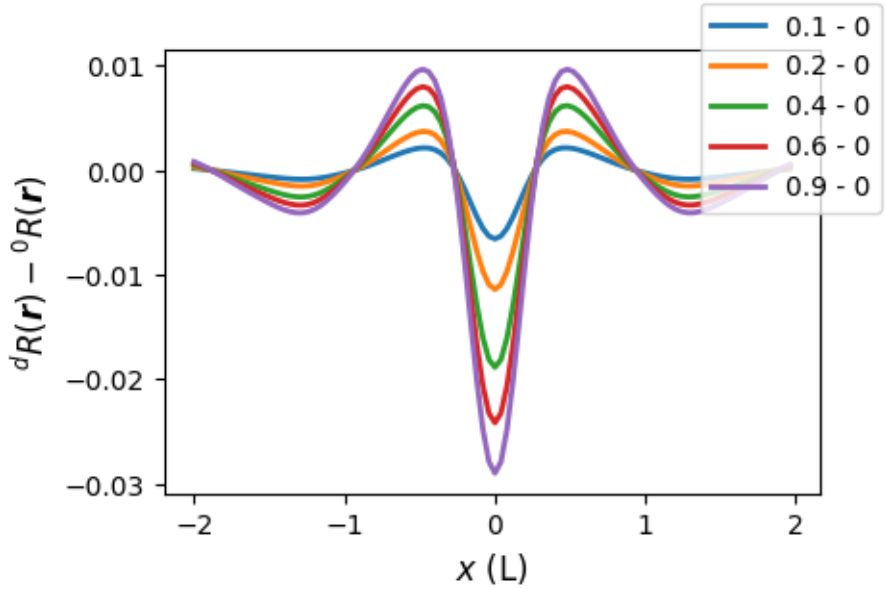

Figure VI: Difference in Wannier functions along the y-axis for different electron interaction strengths.

Figure(VI) shows where the Wannier functions differ, $|{}^d\boldsymbol{R}_1\rangle$ is the ground state with gate

separation d. Electron-electron interactions decrease the probability density near the origin. The biggest increase is at half a unit cell, the highest potential crossed by the line cut. The effect of d on the wave functions is reasonably well described as a single function scaled by a parameter depending on d.

Previous models for the moiré system with a metallic screening gate have used the Hubbard model, a lattice model using Wannier functions as a basis. The Hubbard model has two parameters U and t, which represent the on-site interaction between electrons on a lattice site and the intersite hopping parameter, respectively. The parameter U is naturally expected to reduce in the presence of metallic gates. The modeling performed in this thesis project makes it possible to study the magnitude of this second effect, the renormalization of t due to the screening. t is expected to increase with the overlap of Wannier functions, and the normalization operator Ω_1 can be used as a proxy. We see that the renormalization of Ω_1 by the metallic gate is present here, although relatively small in magnitude.

V. Summary

The discovery of graphene led to an intense period of research on it and other two-dimensional crystals. The construction of Van der Waals heterostructures expands the possible two-dimensional environments in which electrons can be studied. Moirè potentials can arise in these, and they are a promising platform for experiments on many-body electron physics.

This work focused on the modeling of a non-interacting electron gas in a square lattice and the approximation of a square moirè pattern when the Coulomb interaction is strongly screened. Bloch's theorem describes these systems and gives delocalized solutions to the Hamiltonian that split into discrete bands. The Wannier functions form an exponentially localized basis for a set of electron bands similar to atomic orbitals. They are affected by the gauge for the Bloch functions.

In this work, the Bloch functions were computed for a potential on the form $V = V_0 \left(\cos(x) + \cos(y)\right)$. The gauge minimizing spatial extent was computed using gradient descent, giving the maximally localized Wannier functions. For large V, the solutions to a harmonic oscillator were recovered, and for smaller values, the Wannier function spread out over several unit cells.

These Wannier functions were compared to density function theory computations. The non-

interacting case agreed well with weakly interacting functions, and the Coulomb strength smoothly parameterized the Wannier functions.

VI. Outlook

The study of two-dimensional materials and their use as a quantum simulator is an active field of research, and new theoretical tools are needed. The simulations used for this project are inherently limited as they do not account for any electron-electron interactions, which are responsible for most phenomena of interest in moiré materials. The lack of interactions also makes the model computationally cheap, and it was shown to agree well with a more complicated model. In this thesis, only the square lattice was studied, but it is easy to generalize the approach to other two-dimensional lattices, such as the triangular lattice, which is easier to replicate experimentally. The square lattice investigated in this thesis has not yet been experimentally realized. Moirè potentials on this and other lattices promise to become important systems for studying many-body electron physics.

References

[1] I. Bloch, J. Dalibard, and S. Nascimbène, Nature Physics **8**, 267– (2012).

[2] K. Novoselov, A. Geim, S. Morozov, D. Jiang, Y. Zhang, S. Dubonos, I. Grigorieva, and A. Firsov, Science **306**, 666 (2004).

[3] A. Geim and I. Grigorieva, Nature **499**, 419–425 (2013).

[4] Y. Yang, Y. Yang, M. Morales, and S. Zhang, Phys. Rev. B **113**, 035135 (2026).

[5] N. Marzari, A. Mostofi, J. Yates, I. Souza, and D. Vanderbilt, Review in Modern Physics **84**, 1611 (2012).

[6] N. Marzari and D. Vanderbilt, Physical Review B **56** (1997).

[7] A. Pisante, Geometric Partial Differential Equations proceed **CRM Series, vol 15**, 227 (2013).